Firing Control Optimization of Lateral Propellant Impulse Thrusters for Trajectory Correction Rockets

Gao Min, Zhang Yongwei, and Yang Suochang

Electronic Engineering Department, Shijiazhuang Mechanical Engineering College

No.97 Heping West Road, Shijiazhuang, Hebei, 050003, China

Abstract

This paper presents an optimum control scheme of firing time and firing phase angle by taking impact point deviation as optimum objective function which takes account of the difference of longitudinal and horizontal correction efficiency, firing delay, roll rate, flight stability, etc. Simulations indicate that this control scheme can assure lateral thrusters be activated at time and phase angle when the correction efficiency is higher. Further simulations show that the impact point dispersion is mainly influenced by the total impulse deployed, and the impulse, number and firing interval need to be optimized to reduce the impact point dispersion of rockets.

1. Introduction

Dispersion characteristics of the trajectory correction rockets can be dramatically improved by outfitting with a suitable trajectory correction flight control system. A flight control system consists of a finite number of lateral propellant impulse thrusters ("thrusters" for short) mounted forward on the rocket body, computes position and velocity errors through comparing the position and velocity measured by GPS or ground-based radar system with pre-specified (reference) trajectory, and fires thrusters to change velocity direction and assist the rocket to follow a pre-specified trajectory, which can reduces the impact point dispersion and increases the hit probability of rockets.

Research and development on the use of thrusters in order to improve the precision of rockets has been going on for decades. The thrusters' application on rockets has been originally considered by Harkins and Brown [1]. They have proposed a method using a set of thrusters to marginalize the off-axis angular rates of the rockets just after exiting the launcher and managed to reduce the impact point dispersion by the factor of 4. Jitpraphai and Costello [2] have proposed a simplified control system with thrusters and demonstrated that impact point dispersion of a direct fire rocket could be drastically reduced. Recently, Bojan Pavković and Miloš Pavić [3] have presented a simplified control scheme for artillery rockets named the active damping method which performs a correction of disturbances immediately after a rocket exits a launcher tube. It is shown that the application of such a control system achieves a significant dispersion reduction.

Because each thruster imparts a single, short-duration, large force to the rocket in the plane normal to the rocket axis of symmetry, the control scheme of thrusters mainly involves two aspects: the firing time and the firing phase angle. Jitpraphai and Costello [2] compute firing phase angle by the phase angle of trajectory deviation, theoretical analysis shows that this method may not get the best trajectory correction performance under some conditions, and the induced effects of rocket flight time on trajectory performance are not considered. Yang Hongwei [4] converts the problem of determining control parameters of the pulsejets into the design of the experiment with multi-factor and multi-level. Introducing the firing time as a controllable factor, the relationship model among firing time, number of pulsejets and total value of trajectory correction was obtained by using regression analysis. This scheme can determine the firing time and number of pulsejets needed quickly, and reduce the trajectory error of the rocket effectively, but the difference of longitudinal and horizontal correction efficiency is not considered. Cao Yingjun [5] presents an optimization strategy for the firing phase angle, which makes the total number of thrusters minimized for the residual trajectory deviation after previous correction. However, the foremost goal of trajectory correction is to decrease the trajectory error, the consumption number of thrusters should be taken as the secondary factor. In this paper, to reduce the impact point dispersion of a rocket using lateral thrusters coupled to a trajectory flight control system, a 6-DOF trajectory model with lateral force is established, and then the control algorithm of firing time and firing phase angle is put forward with taking impact point deviation as optimum objective function.

2. 6-DOF Trajectory Model with Lateral Force

The numerical simulation is based on a rigid body six degree of freedom model typically utilized in flight dynamic analysis of rockets. Figure 1 shows the rocket configuration with a lateral thruster ring mounted on the forward part of rockets. The thrusters are assumed to be located at l from the center of mass. The 6-DOF trajectory model with lateral force can be established by taking the lateral force and its moment into the ballistic motion equations.

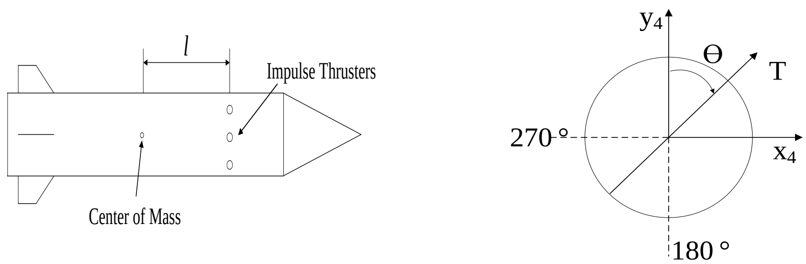

a) Layout of thrusters b) Lateral force

Figure 1: Schematic of layout and lateral force of thrusters

The lateral force in quasi-body reference frame can be described as:

$$\begin{bmatrix} T_{x_4} \\ T_{y_4} \\ T_{z_4} \end{bmatrix} = \begin{bmatrix} 0 \\ T\cos\theta \\ T\sin\theta \end{bmatrix} \quad (1)$$

In equation (1), T is the lateral force of a thruster in quasi-body reference frame, and θ is the phase angle of lateral force.
Using the quasi-body to aero-ballistic reference frame transformation, we can obtain the lateral force in aero-ballistic reference frame:

$$\begin{bmatrix} T_{x_2} \\ T_{y_2} \\ T_{z_2} \end{bmatrix} = \begin{bmatrix} \cos\alpha\cos\beta & -\sin\alpha\cos\beta & \sin\beta \\ \sin\alpha & \cos\alpha & 0 \\ -\cos\alpha\sin\beta & \sin\alpha\sin\beta & \cos\beta \end{bmatrix} \begin{bmatrix} 0 \\ T\cos\theta \\ T\sin\theta \end{bmatrix} \quad (2)$$

In equation (2), α is the angle of attack of the rocket, β is its sideslip angle.
The translational kinetic differential equations of the rocket in aero-ballistic reference frame are given in equation (3).

$$\begin{aligned} \frac{dV}{dt} &= P_{x_2} + F_{x_2} + T_{x_2} \\ V\frac{d\theta'}{dt} &= P_{y_2} + F_{y_2} + T_{y_2} \\ -V\cos\theta'\frac{d\psi_v}{dt} &= P_{z_2} + F_{z_2} + T_{z_2} \end{aligned} \quad (3)$$

The applied loads appearing in equation (3) consist of main rocket thrust (P), lateral thruster force (T), and other forces (F) components. V, θ', and ψ_v are the velocity, flight path angle, and flight path azimuth angle of the rocket, respectively.
Lateral moment in quasi-body reference frame is given by equation (4).

$$\begin{bmatrix} M_{Tx_4} \\ M_{Ty_4} \\ M_{Tz_4} \end{bmatrix} = \begin{bmatrix} 0 \\ -T_{z_4} l \\ T_{y_4} l \end{bmatrix} \tag{4}$$

The rotational kinetic differential equations of the rocket in quasi-body reference frame are given by equation (5).

$$\begin{bmatrix} J_{x_4} \dfrac{d\omega_{x_4}}{dt} \\ J_{y_4} \dfrac{d\omega_{y_4}}{dt} \\ J_{z_4} \dfrac{d\omega_{z_4}}{dt} \end{bmatrix} = \begin{bmatrix} M_{x_4} + M_{Tx_4} \\ M_{y_4} + M_{Ty_4} \\ M_{z_4} + M_{Tz_4} \end{bmatrix} - \begin{bmatrix} 0 \\ \left(J_{x_4} - J_{z_4}\right)\omega_{x_4}\omega_{z_4} \\ \left(J_{y_4} - J_{x_4}\right)\omega_{x_4}\omega_{y_4} \end{bmatrix} + \begin{bmatrix} 0 \\ -J_{z_4}\omega_{z_4} \dfrac{d\gamma}{dt} \\ J_{y_4}\omega_{y_4} \dfrac{d\gamma}{dt} \end{bmatrix} \tag{5}$$

The applied moments appearing in equation (5) contain contributions from lateral thruster forces, M_T , and other forces, M . γ is the Euler roll angle of the rocket. $w_{x_4}, w_{y_4}, w_{z_4}$ are components of the angular rate vector. $J_{x_4}, J_{y_4}, J_{z_4}$ are components of the moment of inertia.
Other motion equations of the rocket do not involves lateral forces or lateral moments can be obtained in [7].

3. The Establishing of Optimum Objective Function

Figure 2 shows the progress of trajectory correction of a thruster. Assumed that M is the target and O is the predicted impact point, the distance between the predicted impact point and the target is OM, the longitudinal and horizontal deviation are ΔL and ΔH respectively. Supposing that the longitudinal and horizontal correction distance of the rocket are P_x and P_z respectively once a thruster is activated, the resulted impact point of the rocket is predicted at A, the distance between the predicted impact point A and the target M is reduced to be AM.

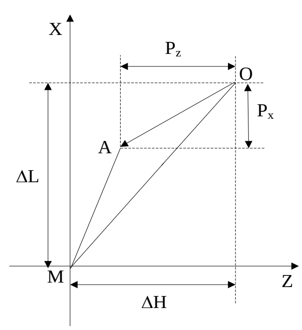

Figure 2: Schematic of trajectory correction

Because the aim of trajectory correction is to reduce the impact point deviation, it is the foremost to make best use of the energy of thrusters to obtain the minimum impact point deviation. Thereafter, the impact point deviation, namely AM, is taken as the objective function for optimization. It is assumed that the plus direction of ΔL and P_x is the X direction in inertia reference frame, and the plus direction of ΔH and P_z is the Z direction in inertia reference frame. AM can be described by equation (6):

$$AM = [(\Delta L + P_x)^2 + (\Delta H + P_z)^2]^{1/2} \tag{6}$$

In equation (6), ΔL and ΔH are decided, so AM mainly relates to P_x and P_z. P_x and P_z depend on roll rate of the rocket, impulse, firing time and firing angle phase of the thruster. In the flight phase, the firing time and firing phase angle are taken as design variables of the objective function while the individual thruster impulse and roll rate of the rocket are determined at the design phase.

4. Optimization of Firing Phase Angle

For a certain ballistic point (namely a certain firing time), the firing phase angle is only the controllable variable of a thruster. To analyze the impact of firing angle on the trajectory correction performance, the lateral force is seen as a constant because the thrusters are active over a very short duration of time, and θ denotes the phase angle of lateral force in quasi-body reference frame. To determine the firing angle phase, the θ for the minimum AM, denoted by θ_m, should be computed firstly. The general method to compute θ is making its value be equal to phase angle of trajectory deviation α, referencing to Figure 3 (a). However, whether or not this method can get the best trajectory correction performance depends on the longitudinal and horizontal correction efficiency (namely as Converting Coefficient) of thrusters.

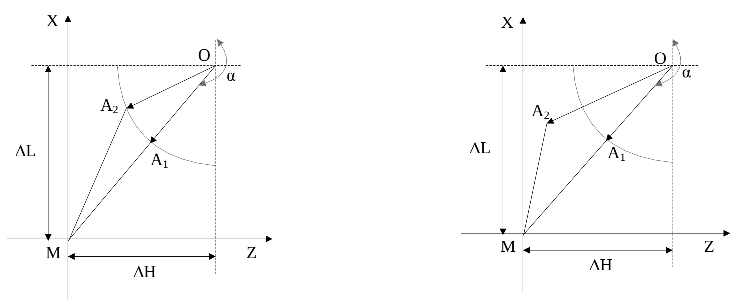

a) With equal converting coefficients b) With unequal converting coefficients

Figure 3: Trajectory correction performance with equal and unequal converting coefficients

Given that the correction distance of a rocket is proportional to impulse of the thruster deployed forward on the rocket body, P_x and P_z can be described by equation (7).

$$\begin{aligned} P_x &= k_x \cdot I \cdot \cos\theta \\ P_z &= k_z \cdot I \cdot \sin\theta \end{aligned} \quad \textbf{(7)}$$

In equation (7), I is the impulse of a thruster. k_x and k_z are longitudinal and horizontal converting coefficients of the rocket. The converting coefficients reflect the correction efficiency of the thruster. The impact of correction efficiency on the objective function will be analyzed under two conditions:

(1) When $k_x = k_z$, longitudinal and horizontal correction efficiency of a thruster are the same for a rocket, then possible impact points after correction of the thruster form a circle around O. Assumed that the correction distances are OA_1 and OA_2, corresponding to $\theta = \alpha$ and $\theta \neq \alpha$, then $OA_1 = OA_2$, and OA_1 has the same direction with OM, referring to Figure 3 (a). Equation (8) can be obtained according to triangle trilateral theorem.

$$OA_1 + A_1M < OA_2 + A_2M \quad \textbf{(8)}$$

Because $OA_1 = OA_2$, so $A_1M < A_2M$. Therefore, when $k_x = k_z$, objective function can get the minimum value with $\theta = \alpha$.

(2) When $k_x \neq k_z$, longitudinal and horizontal correction efficiency of the thruster are not the same, whether or not $OA_1 = OA_2$ is not sure, referring to Figure 3 (b), A_1M may not less than A_2M, namely objective function can not always get the minimum value with $\theta = \alpha$. Under this condition, a new method is required to compute θ_m.

Because an analytic solution is not got by equation (6), θ_m is solved by the binary iteration method given in Figure 4, where $[\theta_1, \theta_2]$ is the solution limits, N is the number of iterations.

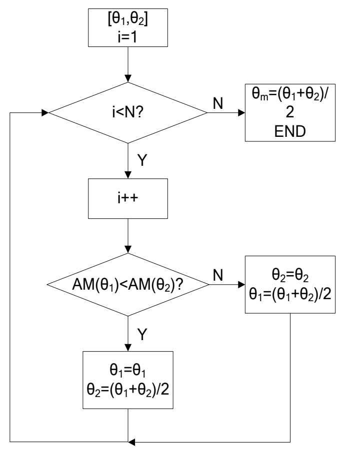

Figure 4: Solution flow of θ_m

To reduce the number of iterations and increase the solution accuracy, solution limits can be got by equation (9).

$$[\theta_1, \theta_2] = \begin{cases} [0^\circ, 90^\circ] & \Delta H < 0, \Delta L < 0 \\ [90^\circ, 180^\circ] & \Delta H < 0, \Delta L > 0 \\ [180^\circ, 270^\circ] & \Delta H > 0, \Delta L > 0 \\ [270^\circ, 360^\circ] & \Delta H > 0, \Delta L < 0 \end{cases} \quad \textbf{(9)}$$

The solution accuracy can reach 0.1 degree with N=10, so θ_m can be solved quickly by this method.

The firing phase angle, denoted by Φ_c, is the phase angle of the thruster in quasi-body reference frame when it gets the firing signal from the control system. Firing time delay and impulse duration time should be taken into account to make sure the average angle of lateral force equal to θ_m.

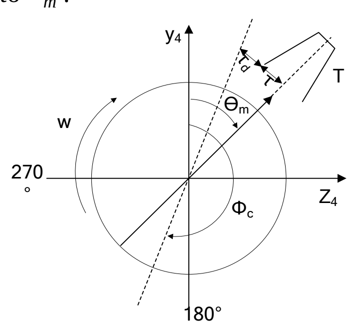

Figure 5: Schematic of firing phase angle

Schematic of firing phase angle is given in Figure 5. The relation between firing phase angle Φ_c and θ_m is given by equation (10).

$$\Phi_c = \theta_m + \pi - \omega(\tau_d + \tau) \tag{10}$$

In equation (10), τ_d is the firing delay, τ is a half of the impulse duration. ω is the roll angular rate.
When the phase angle Φ of the thruster will be activated is equal to the firing phase angle, the thruster can be activated, namely the condition to activate a thruster is:

$$|\Phi - \Phi_c| \le \varepsilon \tag{11}$$

In equation (11), ε is the desired activation threshold.

5. Optimization of Firing Time

After the optimization of firing phase angle, the other controllable variable of objective function is the firing time of thrusters. The general firing time control algorithm has two strategies:
(1) Time elapsed from the previous thruster firing must be longer than a specified duration Δt_{fire}:

$$t - t^* > \Delta t_{fire} \tag{12}$$

In equation (12), t^* is the firing time of the previous thruster.
(2) If predicted impact point deviation is greater than a specified distance, activate the thruster as soon as possible.
Δt_{fire} is an important design parameter of thrusters. If it is set too low, the rocket does not have sufficient time to respond and too many thrusters will be fired, tending to over-compensate for trajectory deviation. Simultaneously, a lower Δt_{fire} may have an impact on the flight stability of the rocket. On the other hand, if it is set too high, only a small number of thrusters can possibly be fired and the capabilities of the residual thrusters will be wasted.
The impact of flight time on trajectory correction performance of thrusters is not considered by strategy (2), which may lead to that thrusters are activated at the time when the correction efficiency is lower. Gao Feng [6] gave the conclusion that the longitudinal correction efficiency of thrusters is lower in ballistic ascending segment of the rocket, and longitudinal and horizontal correction efficiency reduces with flight time in ballistic descending segment. Simulation results of Converting Coefficients of a rocket have been shown in Figure 6.

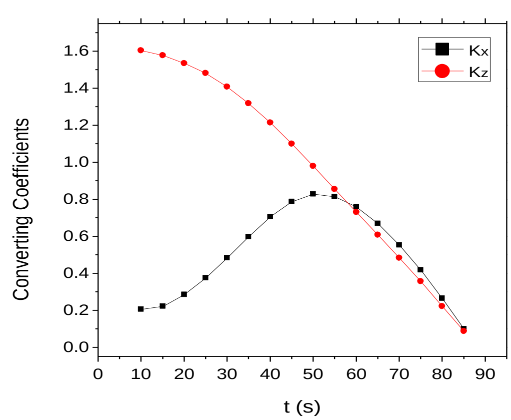

Figure 6: Converting coefficients vs. flight time

It can be known from equation (6) and Figure 6 that the value of the objective function (activated at the optimized firing phase angle) tends to increase in ballistic descending segment. Supposing that t_k is the time of ballistic vertex, the value of the objective function at t_k can be taken as a reference value, denoted by $AM(t_k)$. In ballistic ascending segment, thrusters can be activated if the value of the objective function is less than the reference value $AM(t_k)$, otherwise can't. This method can guarantee that thrusters be activated at the time when correction efficiency is higher, especially in the ballistic ascending segment.
To sum up, the firing time control algorithm can be improved as followed equation (13).

$$\begin{aligned} & t-t^{*} > \Delta t_{fire} \\ & AM(t) < AM(t_k) \quad t < t_k \\ & AM(t) < OM(t) \quad t \ge t_k \end{aligned} \tag{13}$$

In equation (13), t_k is the time of ballistic vertex.

6. Results and Discussion

To investigate the correction performance of thrusters and verify the effectiveness of the firing control scheme, some simulations of a rocket have been done by numerical integration of the equations described above using a fourth order Runge-Kutta algorithm. The rocket configuration used in the simulation study is a representative 122 mm artillery rocket, 2.99 m long, fin-stabilized, with four pop-out fins on its rear part. The main rocket motor burns for 2.55s and imparts an impulse to the rocket of 54247 N-s. During the main rocket motor burn, the forward velocity of the rocket is increased from 46.9m/s to 935.7m/s. The rocket weight, mass center location from the nose tip, roll inertia, and pitch inertia before and after burn is 66.1/43.0 kg, 1.43/1.21 m, 0.16/0.12 kg-m2, and 48.42/36.36 kg-m2, respectively. The rocket is launched at sea level toward a target on the ground with altitude and cross range equal zero at a range of 28100 m. The thrust ring is assumed to be located at 0.869 m from the nose tip of the rocket, and contains 50 individual thrusters where each individual thruster imparts an impulse of 15 N-s on the rocket body over a time duration of 0.02s. The minimum firing interval of thrusters Δt_{fire} is set to 0.2s. The desired activation threshold ε is set to 3° .

The time-varying data of uncontrolled and controlled trajectories with optimum firing control scheme against a nominal command trajectory for the example rocket are compared in Figure 7.
Figure 7 (a) plots the total number of thrusters fired vs. time. 5 thrusters are fired in 10~15s, and 43 thrusters are fired in 45~70s. No thrusters are fired in 15~45s indicates that the correction efficiency is relatively low during this period. No thrusters are fired after 70s because the predicted impact point deviation is too small to implement any trajectory correction. The activation of thrusters will arouse the increase of attack angle of rocket, as shown in Figure 7 (b).
It can be known from Figure 7 (c) and Figure 7 (d) that the predicted longitudinal and horizontal impact point deviations reduce gradually. The horizontal impact point deviation reduces quickly, while longitudinal impact point deviation has no significant change in 10~20s, indicates that the thrusters fired in this period are used for horizontal correction, corresponding to the fact that the horizontal correction efficiency of thrusters in this period is higher (k_z is greater, referencing to Figure 5). Both horizontal and longitudinal impact point deviation reduce quickly in 45~70s, indicates that thrusters fired in this period are used for both horizontal and longitudinal correction, corresponding to the fact that the horizontal and longitudinal correction efficiency in this period are similar ($k_x \approx k_z$).
Figure 7 (e) and Figure 7 (f) show that the trajectory correction rocket flights to target point gradually under the effect of thrusters. The final impact point deviation of the rocket were reduced from horizontal 341.3m and longitudinal 483.3m in the uncontrolled case to horizontal 10.9m and longitudinal 15.9m in the controlled case, which demonstrates the firing control scheme works effectively.

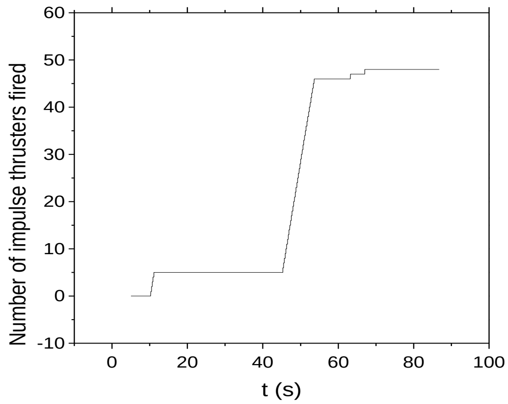

a) Total number of thrusters tired vs. time

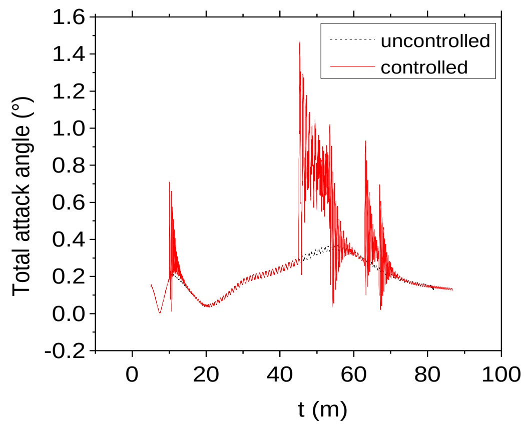

b) Total attack angle vs. time

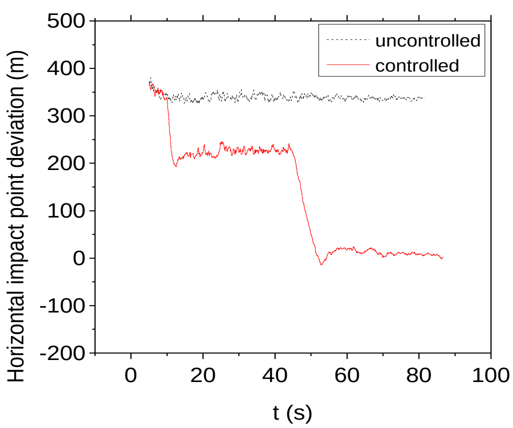

c) Horizontal impact point deviation vs. time

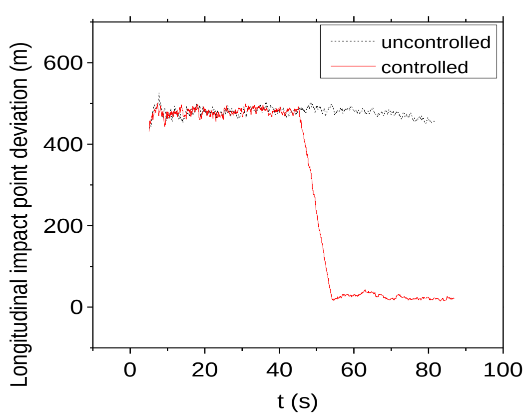

d) Longitudinal impact point deviation vs. time

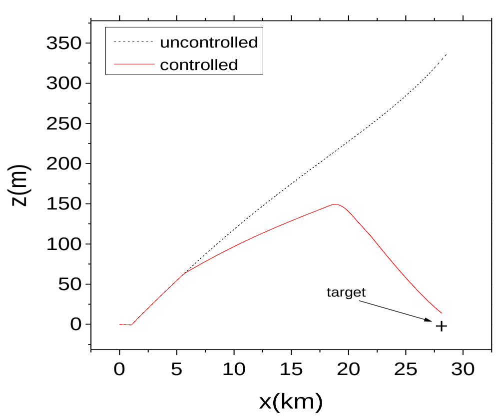

e) Cross range vs. range

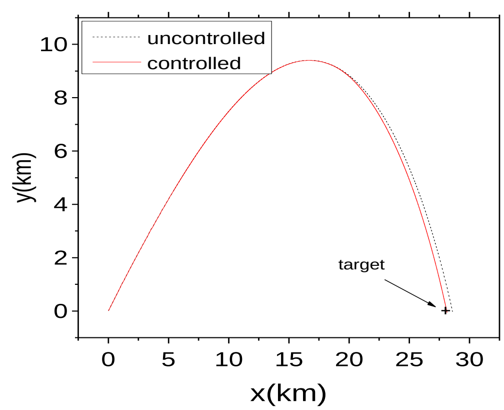

f) Altitude vs. range

Figure 7: Correction performance of the optimum firing control scheme

Figure 8 shows the impact point distribution using the Monte Carlo method. The cases of the uncontrolled rockets as well as of the rockets with general firing control scheme and optimum firing control scheme are shown. The analysis was performed for a statistical sample of 1024 simulations.

As shown in Figure 8, impact point distribution of the trajectory correction rockets reduces greatly. The rockets with the general firing control scheme have a CEP of 38m, while the CEP of rockets with the optimum firing control scheme is 20m. The average thruster consumption and its standard deviation of the rockets with the general firing control scheme are 31.7 and 15.5, while the average thruster consumption and its standard deviation of the rockets with the optimum firing control scheme are 25.1 and 13.3. The decrease of impact point dispersion of rockets and the reduction of thruster consumption testify the effectiveness of firing control optimization.

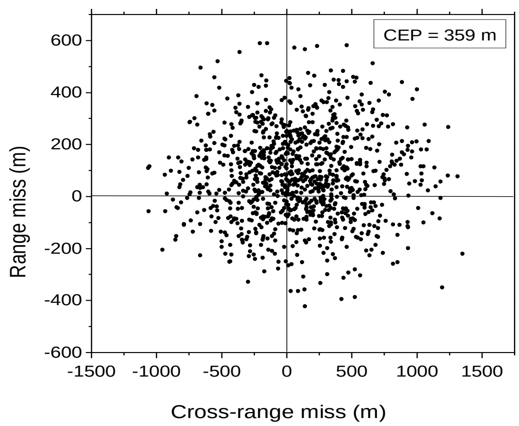

a) Impact point distribution of uncontrolled rockets

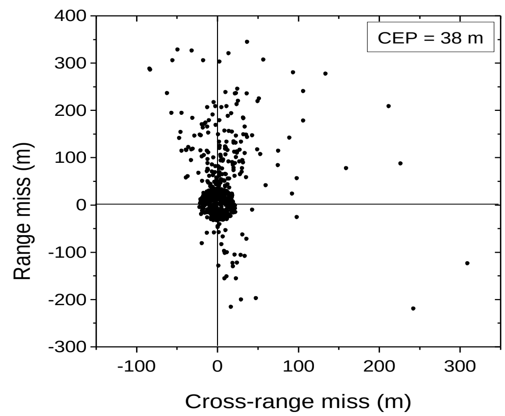

b) Impact point distribution of rockets with general firing control scheme

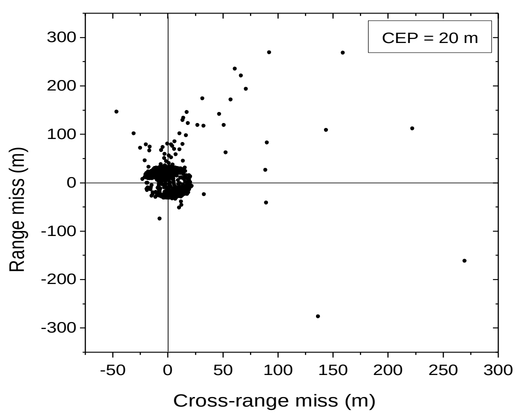

c) Impact point distribution of rockets with the optimum firing control scheme

Figure 8: Impact point distribution

Figure 9 shows the impact of thruster parameters on the CEP and flight stability of rockets. Figure 9 (a) shows the relation between CEP of rockets, number of thrusters mounted on rocket, and individual thruster impulse. It can be known that the CEP of rockets is highly correlated with the number of thrusters and individual thruster impulse, CEP reduces steadily as the number of thrusters or individual thruster impulse is increased. Figure 9 (b) shows the relationship between CEP of rockets, individual thruster impulse, and the total impulse of thrusters. For a value of the total impulse, as the individual thruster impulse is increased, the number of thrusters decreases proportionally to remain the total impulse as a constant. As shown in Figure 9 (b), CEP reduces gradually as the total impulse is increased, the value of individual thruster impulse has a small impact on CEP.

Figure 9 (c) shows the relationship between maximum total attack angle, individual thruster impulse, and the minimum firing interval (Δt_{fire}). The results indicate that individual thruster impulse and minimum firing interval have a direct impact on the maximum total attack angle, as individual thruster impulse increases or minimum firing interval reduces, the maximum total attack angle increases, which may affect the flight stability of trajectory correction rockets.

Based on the above discussion, some suggestions are put forward to determine the thruster configuration parameters of trajectory correction rockets. Firstly, the total impulse should be determined according to CEP needed, because the impact point dispersion is mainly influenced by the total impulse of lateral thrusters deployed. Secondly, individual thruster impulse should be determined according to the total impulse, limits of layout space on the rocket, flight stability of rockets, cost, etc. If the individual thruster impulse is too small, there may be too many thrusters need to be mounted on the rocket. On the other hand, if the individual thruster impulse is too large, the flight stability may deteriorated. Thirdly, the minimum firing interval should be determined according to the individual thruster impulse, flight stability of rockets, correction efficiency of thrusters, etc. If the individual thruster impulse is large, a relatively large minimum firing interval should be set to guarantee the flight stability of rockets. If the individual thruster impulse is small, a relatively small minimum firing interval time should be set to insure thrusters can be activated at the segment of trajectory while the correction efficiency is higher.

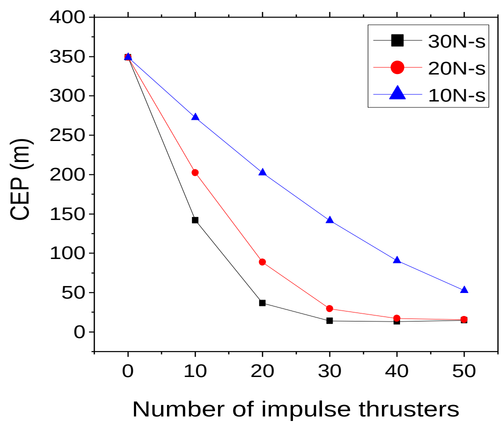

a) CEP vs. number of thrusters and individual thruster impulse

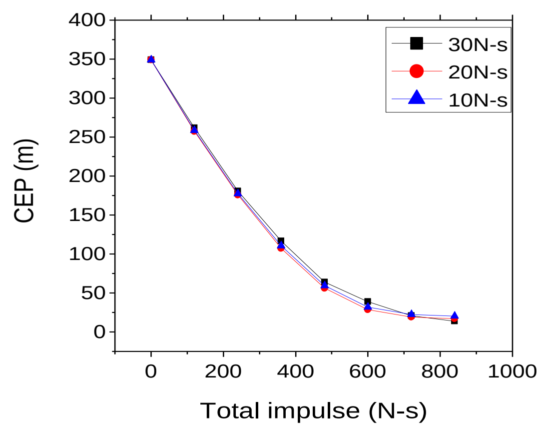

b) CEP vs. total impulse of thrusters and individual thruster impulse

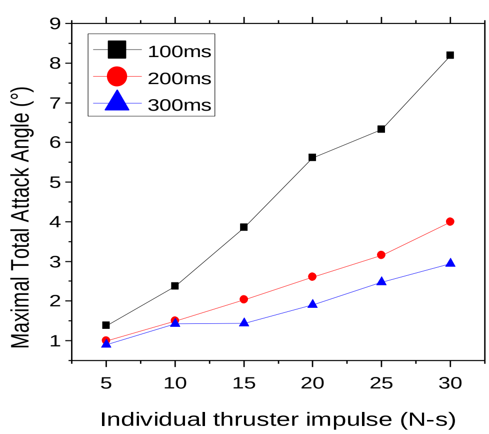

c) Maximal total attack angle vs. individual thruster impulse and minimum firing interval

Figure 9: The impact of parameters of thrusters on CEP and flight stability of rockets

7. Conclusion

This paper establishes the 6-DOF trajectory model of a rocket with lateral force, and presents an optimum control scheme of firing time and firing phase angle by taking impact point deviation as optimum objective function which takes account of the difference of longitudinal and horizontal correction efficiency, firing delay, roll rate, flight stability, etc. Simulations indicate that this control scheme can assure lateral propellant impulse thrusters be activated at time and phase angle when the correction efficiency is higher. The variations of rocket impact point dispersion are analyzed with different impulse and number of lateral propellant impulse thrusters. It is shown that the impact point dispersion is mainly influenced by the total impulse of lateral propellant impulse thrusters deployed, and steadily decreases as the total impulse is increased. The impulse, number and firing interval need to be optimized to insure the flight stability of rockets and lateral propellant impulse thrusters activated at time when the correction efficiency is higher.

References

[1] Harkins,T., and Brown,T. Using Active Damping as a Precision-Enhancing Technology for 2.75-inch Rockets. ARL-TR-1772, U.S. Army Research Laboratory, Aberdeen Proving Ground, MD, 1999.

[2] Jitpraphai,T., and Costello,M. Dispersion Reduction of a Direct Fire Rocket Using Lateral Pulse Jets. *Journal of Spacecraft and Rockets*, Vol.38, No.6, 2001, pp.929-936.

[3] Bojan Pavković, Miloš Pavić, and Danilo ĆukW. Enhancing the Precision of Artillery Rockets Using Pulsejet Control Systems with Active Damping. *Scientific Technical Review*, Vol. 62, No. 2, 2012, pp.10-19.

[4] Yang Hongwei, Dou Lihua, and Gan Minggang. Control Method of Impulse Actuator of Antiaircraft Trajectory Correction Projectile. *Transactions of Beijing Institute of Technology*, Vol.31, No.10, 2011, pp.1184-1188.

[5] Cao Yingjun, Yang Shuxing, and Li Xingjun. Research on Firing Phase Angle Optimization of Terminal Trajectory Correction Projectile Based on Pulse Jet Control. *ACTA ARMAMENTARII*, Vol.29, No.8, 2008, pp.897-901

[6] Gao Feng, and Zhang He. Study of 2-D Trajectory Correction Based on Geomagnetic Detection with Impulse Force for Projectiles. *Journal of System Simulation*, Vol.23, No.1, 2011, pp. 123-128.

[7] Qian Xingfang, Lin Ruixiong, and Zhao Yanan. Aerothermodynamics of Missile Flight. Beijing Institute of Technology Press, Beijing, 2008, pp. 36-48.